Journal of Hazardous Materials 187 (2011) 89–95

Contents lists available at ScienceDirect

Journal of Hazardous Materials

journal homepage: www.elsevier.com/locate/jhazmat

Kinetics and mechanism of arsenate removal by nanosized iron oxide-coated perlite

M.G. Mostafa [a], Yen-Hua Chen [b], Jiin-Shuh Jean [b,*], Chia-Chuan Liu [b], Yao-Chang Lee [c]

[a] Institute of Environmental Science, University of Rajshahi, Rajshahi 6205, Bangladesh
[b] Department of Earth Science, National Cheng Kung University, Tainan 701, Taiwan
[c] National Synchrotron Radiation Research Center, Hsinchu, Taiwan

ARTICLE INFO

Article history:
Received 20 July 2010
Accepted 23 December 2010
Available online 5 January 2011

Keywords:
Arsenate
Adsorption
Nanosized iron oxide
Perlite
Kinetics

ABSTRACT

This study discussed the adsorption kinetics of As(V) onto nanosized iron oxide-coated perlite. The effects of pH, initial concentration of As(V) and common anions on the adsorption efficiency were also investigated. It was observed that a 100% As(V) adsorption was achieved at pH value of 4–8 from the initial concentration containing 1.0 mg-As(V) L^{-1} and the adsorption percentage depended on the initial concentration; the phosphate and silicate ions would not interfere with the adsorption efficiency. Furthermore, nanosized iron oxide-coated perlite (IOCP) has been shown to be an effective adsorbent for the removal of arsenate from water. The adsorption kinetics were studied using pseudo-first- and pseudo-second-order models, and the experimental data fitted well with the pseudo-second-order model. Moreover, it suggests that the Langmuir isotherm is more adequate than the Freundlich isotherm in simulating the adsorption isotherm of As(V). The adsorption rate constant is 44.84 L mg^{-1} and the maximum adsorption capacity is 0.39 mg g^{-1}. These findings indicate that the adsorption property of IOCP gives the compound a great potential for applications in environmental remediation.

1. Introduction

Arsenic contamination in groundwater has become a serious threat to environmental and human health. It has been found in groundwater in many parts of the world where a large number of people have already been affected with various diseases. Arsenic (As) is considered as a highly toxic element and abundant in our environment with both natural and anthropogenic sources [1].

A number of techniques, namely coagulation, precipitation, filtration, reverse osmosis, ion exchange, and adsorption have been used to remove toxic elements including arsenic from aquatic environment [2–6]. Recently iron oxide is applied to adsorb arsenic and heavy metals from water. The adsorption technique is better capable of removing heavy metals over a wide pH range and even in low concentrations than the precipitation method [7,8]. Hydrous ferric oxide (HFO) has been extensively studied as a promising adsorption material for removing both arsenate and arsenite from aqueous media [9]. It is also reported that the removal of As(V) from groundwater using nano-scale zero-valent iron (NZVI) has a high efficiency [10]. The results showed that about 100% As(V) removal was achieved in 10 min of adsorption reaction. However, this kind of materials are usually made as suspensions in aqueous solution and are available only as fine powders. Therefore, it is not suitable to use these fine powders in column applications because of their low hydraulic conductivity [11,12].

Perlite is cheap and naturally occurring volcanic silicates. Perlite is mainly composed of silica, aluminum, potassium and sodium and has been extensively used for the adsorption of heavy metals including Cd, Cu(II), Cr(III) and some organic solutes such as CTAB methylene and p-chlorophenol [13–19]. So far of our knowledge, there is no report of using any other forms of perlite for adsorbing arsenic species from aqueous medium. This study considers perlite could be used as an adsorbent material due to its high porosity, surface area, low cost and natural availability. A simple and economic preparation of the iron oxide-coated perlite (IOCP) adsorbent was performed. The purpose of this study was to evaluate the maximum adsorption capacity and to study the mechanism of As(V) adsorbed on the iron oxide- coated perlite (IOCP). The adsorption kinetics, isotherms, and maximum adsorption capacity are discussed.

2. Materials and methods

2.1. Preparation of adsorbent

Perlite (beads, grade 5, Sigma–Aldrich) was soaked in H_2SO_4 solution at pH 1 for 24 h and then rinsed 3–4 times with deionized

* Corresponding author at: No. 1, University Road, Tainan City 701, Taiwan. Tel.: +886 62757575x65426; fax: +886 62740285.
E-mail address: jiinshuh@mail.ncku.edu.tw (J.-S. Jean).

0304-3894/$ – see front matter © 2011 Elsevier B.V. All rights reserved.
doi:10.1016/j.jhazmat.2010.12.117

water and dried in an oven at 105 ± 1 °C for another 24 h. Thus the perlite with acidic treatment was used for coating application. The solution of Fe(III) was prepared by dissolving reagent grade $FeCl_3 \cdot 6H_2O$ in deionized water. The Fe(III) solution was taken in a beaker, stirring with a magnetic stirrer at 200 rpm and added with 0.5 M NaOH solution until pH at 9.5 ± 0.1 and the Fe(III) solution was continued to mix for 5 min. Subsequently the mixed solution was poured into 100 g perlite in a conical flask and then it was placed in a temperature-controlled shaker at 60 ± 1 °C at 200 rpm for 24 h and finally it was dried in an oven at 105 ± 1 °C for 24 h. After that, the sample was washed 5–7 times with deionized water and finally dried at 60 ± 1 °C.

2.2. Characterization of adsorbent

The particle size of the synthesized iron oxide was determined by the Bruker D8 Advance X-ray diffraction Analyzer (Karlsruhe, Germany). Electron probe micro-analyzer and elemental mapping were used to measure the elemental constitution of the samples. The surface morphology including roughness, cracks, and pore distribution of perlite, ICOP, and As(V)-treated ICOP were analyzed by environmental scanning electron microscopy/energy dispersive X-ray (ESEM-EDAX, FEI, Quanta 400F, USA). The specific surface area, micropore volume and average pore diameter of the samples were measured by the BET analyzer (Beckman Coulter, Model SA 3100) (Brea, CA, USA); the BET and Dubinin–Radushkevich (D–R) equations were used to determine the surface area and volumes of the micropores, respectively [20]. FTIR analysis was used to measure the chemical bonding nature of As(V) on the IOCP surface (Thermo Nicolet, Magna-IR 860); the samples were diluted to a concentration of 2% with IR-grade KBr.

2.3. Batch experiments of As(V) adsorption

Batch adsorption of As(V) was carried out in a 125-mL pyrex conical flask containing 1 g IOCP adsorbent in the 50 mL reaction solution. The initial As(V) solution concentrations of 0.2, 0.5, 1.0, and 1.5 mg L^{-1} in 0.01 M NaCl solution were used and the pH value was 6.5–7. The pH of the solution was adjusted using 0.1 M HCl and 0.1 M NaOH solutions during the adsorption study. The samples were collected at different intervals of time from 1 min to 1440 min. The solutions were shaken at 200 rpm in a temperature-controlled shaker with the temperature at 30 ± 1 °C. Finally, collected samples were centrifuged in a high speed centrifuge and filtered through 0.2 μm cellulose nitrate membrane filters. The concentrations of As(V) in the samples were determined by Millennium Excalibur Fluorescence Atomic Analyzer (PS Analytical Ltd., Kent, UK) with the detection limit of 0.2 μg L^{-1}.

2.4. Adsorption isotherm

The adsorption isotherm is fundamentally important to evaluate the adsorption capacity and to investigate the characteristics of adsorption. Both the Langmuir and Freundlich adsorption isotherms are known to obtain the adsorption mechanism and maximum adsorption capacity on the adsorbent surface. The Langmuir sorption isotherm equation is given as follows:

$$q_e = \frac{q_m K C_e}{(1 + K C_e)} \quad \text{or} \quad \frac{C_e}{q_e} = \frac{1}{q_m k} + \frac{C_e}{q_m} \tag{1}$$

where q_e (mg g^{-1}) and q_m are the adsorbed amount and maximum adsorbed amount of arsenic by IOCP, respectively, K is the Langmuir isotherm constant related to binding energy, and C_e is the equilibrium concentration (mg L^{-1}).

Table 1
Particle size of synthesized iron oxides estimated by X-ray diffraction.

2θ	hkl	Particle size (nm)
24.20	012	26.05
33.20	104	22.54
35.68	110	45.95
40.91	113	25.84
49.51	024	20.79
54.11	116	23.84
55.80	108	11.78
62.49	214	34.80
64.05	300	25.70

The empirical Freundlich equation based on sorption onto a heterogeneous surface is given as:

$$q_e = K_F C_e^{1/n} \tag{2}$$

where K_F and n are the Freundlich constants for the system, which were indicators of adsorption capacity and intensity, respectively [21].

2.5. Adsorption kinetics

The pseudo-first-order equation and pseudo-second-order equation are used to illustrate the adsorption kinetics of the adsorbent surfaces; the pseudo-first-order equation can be presented in the form [22,23]:

$$\frac{dq_t}{dt} = K_1(q_e - q_t) \quad \text{or} \quad \ln(q_e - q_t) = \ln q_e - K_1 t \tag{3}$$

where K_1 (min^{-1}) is the rate constant of pseudo-first-order adsorption, q_e (mg g^{-1} of dry weight) is the amount of metal ion sorbed at equilibrium state, and q_t (mg g^{-1} of dry weight) is the amount of metal ion on the surface of the sorbent at any time t (min).

The pseudo-second-order equation can be written as [24]:

$$\frac{dq_t}{dt} = K_2(q_e - q_t)^2 \quad \text{or} \quad \frac{t}{q_t} = \frac{1}{k_2 q_e{}^2} + \frac{1}{q_e} t \tag{4}$$

where K_2 (g mg^{-1} min^{-1}) is the rate constant of pseudo-second-order adsorption.

3. Results and discussion

3.1. Characterization of IOCP and IOCP-As(V) adsorbents

The crystal structure and particle size of the synthesized iron oxide were determined by X-ray diffraction (XRD) analysis. It is observed that the iron oxide has a hematite structure with a pure polycrystalline phase. The Scherrer equation is used to estimate the particle size of the iron oxide, which can be written as:

$$D = \frac{0.9\lambda}{\beta \cos\theta} \tag{5}$$

where D is the particle size in nm, λ is the wavelength of X-ray, β is the full width at the half maximum (FWHM) and θ is the diffraction angle. The details are listed in Table 1 and an average particle size of the iron oxide used in this study is 26.37 nm.

Specific surface areas and pore volumes of the samples were determined using the BET analysis. The specific surface area, pore volume, and average pore diameter of perlite and IOCP are 1.73 m^2 g^{-1}, 2.29 mm^3 g^{-1}, 19 Å and 9.26 m^2 g^{-1}, 13.58 mm^3 g^{-1}, 56.5 Å, respectively (Table 2). The results indicate that the specific surface area, pore volume, and average pore diameter of perlite were increased after thermal coating with iron oxide, resulting in the increase of As(V) sorption onto IOCP.

Table 2
Specific surface area of perlite, IOCP and As(V)-adsorbed IOCP.

	Perlite	IOCP	As(V)-adsorbed IOCP
Surface area ($m^2\ g^{-1}$)	1.73	9.62	5.47
Pore volume ($mm^3\ g^{-1}$)	2.29	13.58	6.39
Average pore diameter (Å)	19	56.50	47

BET results suggest that the IOCP has higher specific surface areas and more micropores. Moreover, specific surface area and pore volume of As(V) adsorbed IOCP become lower comparing with the IOCP sample. It suggests that As(V) is adsorbed on the surface of IOCP capable of reducing the surface area and pore volume of IOCP. The average pore diameters of perlite, IOCP, and the As(V)-adsorbed IOCP are 53, 56.5 and 47 Å, respectively. The results indicate that the pore diameter increases with the thermal coating process and decreases with arsenic adsorption on the pore surfaces.

ESEM images were taken at 500× magnifications for the solid samples of perlite, IOCP, and As(V)-adsorbed IOCP (Fig. 1). The result shows that perlite has a rough surface. Cracks and pores are observed on the IOCP surface; however, spots are appeared after coated with iron oxides. Fig. 1C–E shows different surface morphologies of the As(V) adsorbed IOCP samples, where the cracks on the surface increase with increasing initial concentrations of As(V). The EDAX spectra reveal that Fe, Si, Al, Na, K and O signals are existed in IOCP (Fig. 2A), where As(V) signal appears along with other elements after treated with As(V) solution (Fig. 2B). Thus EDAX analysis confirms the presence of As(V) on the adsorbed IOCP surface.

The bonding nature of arsenate adsorbed on the IOCP was examined by FTIR. It is reported that the spectra of arsenate adsorbed on granular ferric hydroxide (GFH) exhibits two absorption bands at 880–890 cm^{-1} and 825–839 cm^{-1} [25]. The higher vibrational frequency band at 880–890 cm^{-1} and the lower vibrational frequency at 825–839 cm^{-1} are assigned to As–O stretching vibration of a bidentate and a monodentate complex of $(FeO)_2AsO_2$, respectively. In our study, the frequency at 890 cm^{-1} and 825 cm^{-1} are observed which indicates that both bidentate and monodenate complex with As–O bonds in $(FeO)_2AsO_2$ on to the IOCP surface (Fig. 3). There-

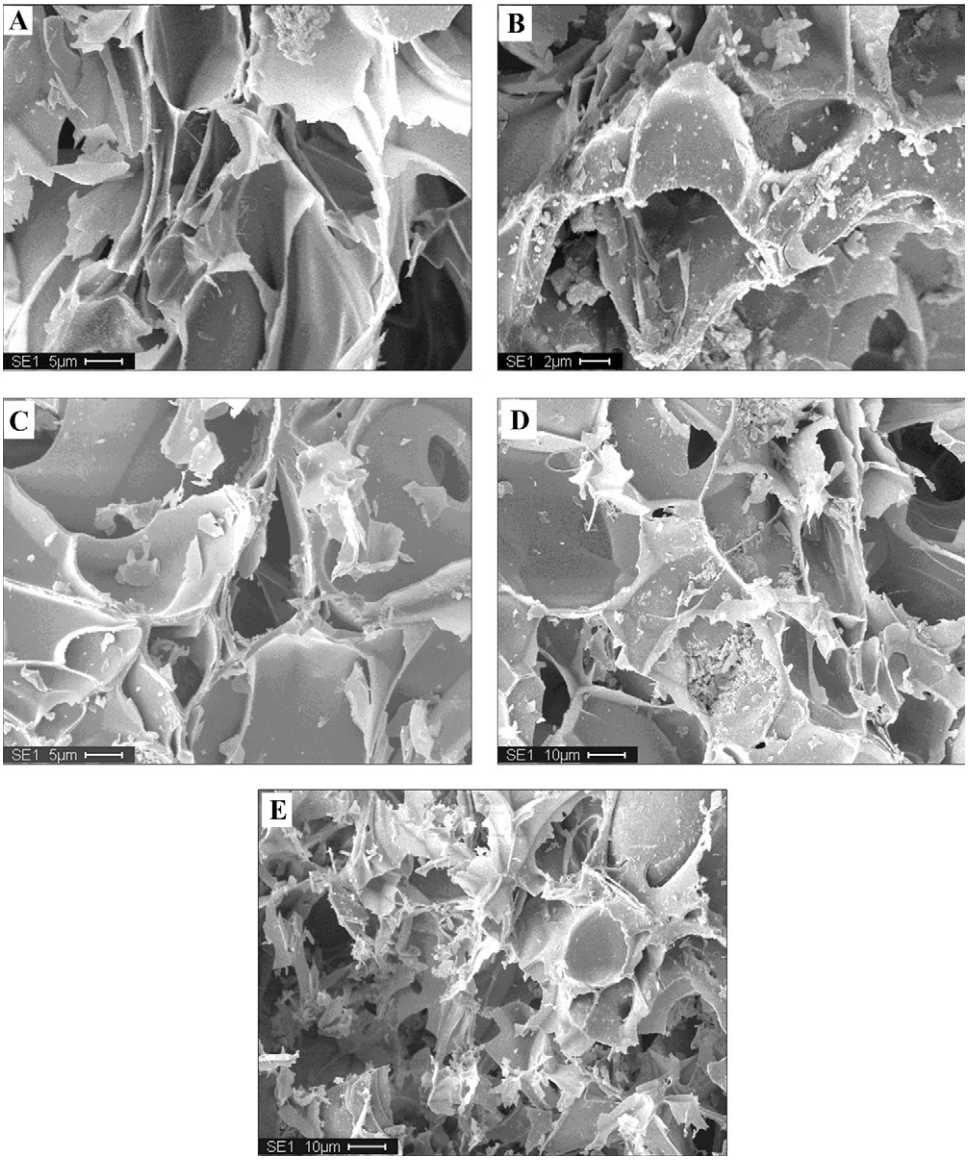

Fig. 1. (a) ESEM images of perlite, (b) IOCP, (c) As(V)-500 ppb treated IOCP, (d) As(V)-1000 ppb treated IOCP and (e) As(V)-1500 ppb treated IOCP. Adsorption conditions: As(V) in 0.01 M NaCl at pH 6.5–7 and adsorbent dose of 10 g L^{-1}.

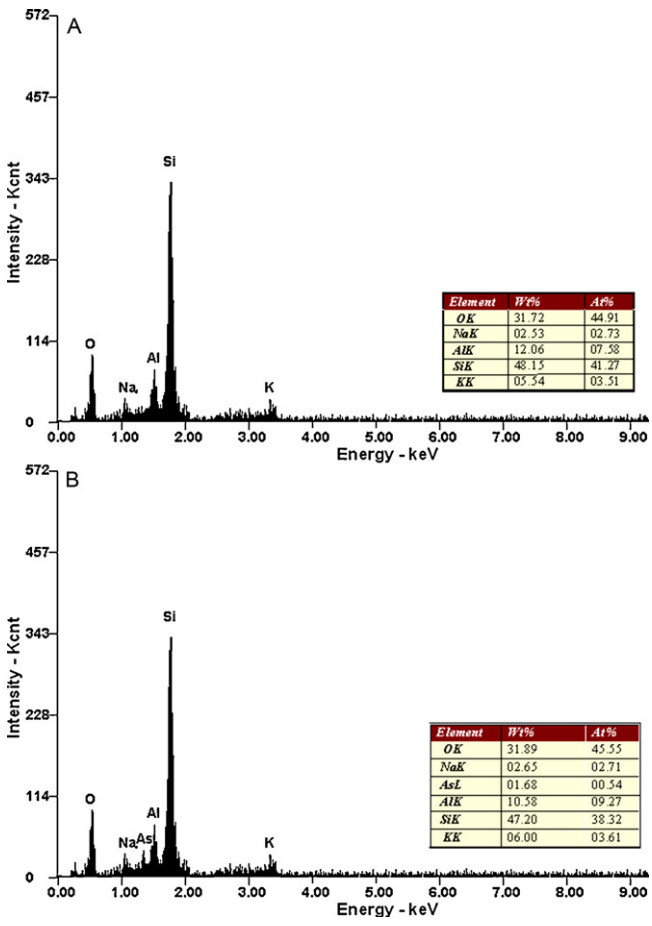

Fig. 2. (a) EDAX spectra of IOCP and (b) As(V)-adsorbed IOCP.

fore, the stretching vibrational frequency of the As–O group in solid phases containing arsenate species appears in the same vibrational frequencies as in Gregg et al. [25]. EDAX and FTIR analyses reveal that the arsenate can be adsorbed onto IOCP. Besides, the results show that arsenic ions are chemisorbed on to the surface of IOCP. It is suggested that As(V) is appeared on the IOCP surface and As(V) species maybe become a constituent of the solid adsorbent.

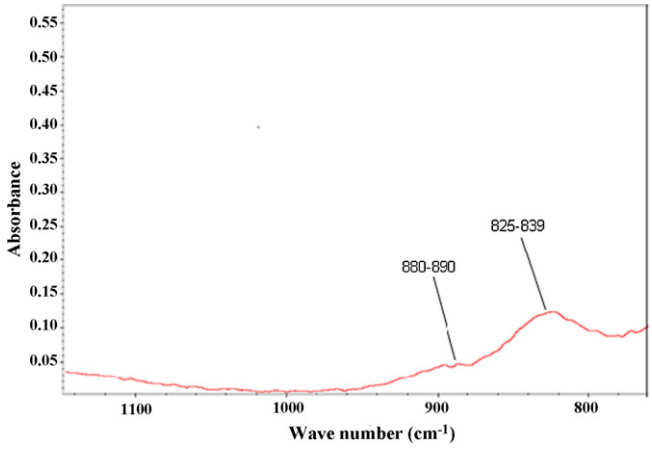

Fig. 3. FTIR spectra of IOCP after treated with As(V) solution. Adsorption conditions: adsorbent dose: 1.0 g–IOCP L^{-1} in 0.01 M NaCl at pH 6.5–7, temperature 30 °C and reaction time 24 h.

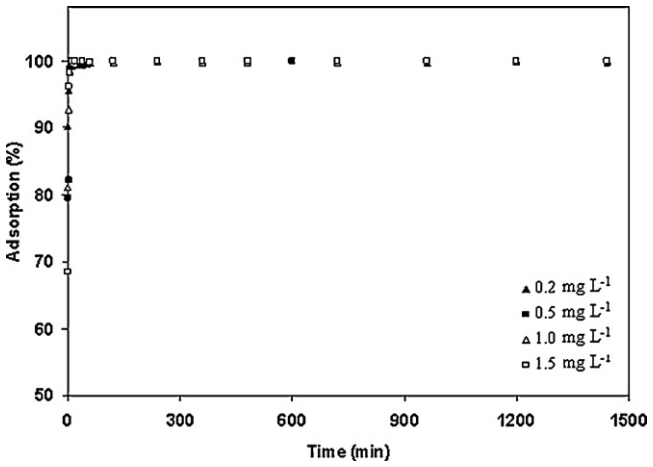

Fig. 4. Adsorption of As(V) as a function of time. Adsorption conditions: 10 g L^{-1} of IOCP in 0.01 M NaCl at pH 6–7 and 30 °C.

3.2. Arsenic adsorption

Fig. 4 presents the adsorption of As(V) on the IOCP adsorbent surfaces for 0.2–1.5 mg L^{-1} of different initial As(V) concentrations at 30 °C, which reveals that adsorption percentage of As(V) increases with increasing time. The adsorbed amount of As(V) increases very rapidly during the first 3 min and then slowly reaches equilibrium around 5 min for all initial As(V) concentrations. About 100% of As(V) removal is achieved within 5 min for all initial As(V) concentrations (up to 1.5 mg L^{-1}). It is observed that the available sites of adsorption become fewer with increasing the initial As(V) concentrations and hence the adsorption percentage depends on the initial concentration, but the equilibrium time is independent on initial concentrations.

3.3. pH effect on adsorption

The dependency of pH on arsenate adsorption is shown in Fig. 5. The adsorbent has a high capacity in a wide pH range from 4 to 10. About 100% adsorption of As(V) is achieved at pH between 4 and 8 and it decreases to 91.12% at pH 10 and 77.25% at pH 12. The maximum adsorption capacity is observed near neutral pH and sharply decreases beyond pH 10. It indicates that the amount of adsorption drops in a higher pH region due to the increase of negative-charge sites on the adsorbent surfaces.

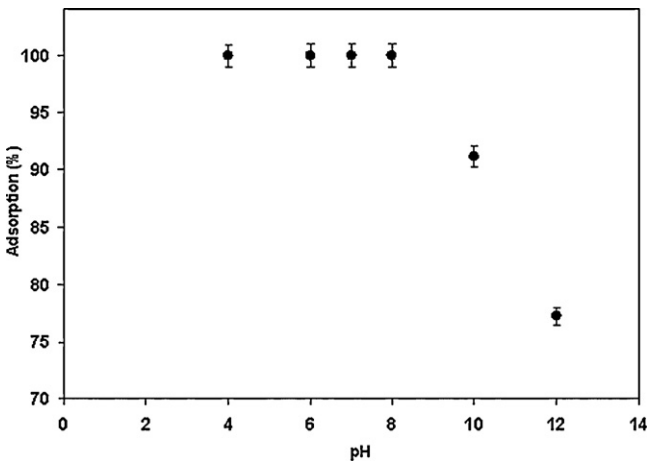

Fig. 5. Adsorption of As(V) on IOCP as a function of pH values. Adsorption condition: 1 mg L^{-1} As(V) adsorbed on 10 g L^{-1} IOCP in 0.01 M NaCl for reaction time of 24 h.

Table 3
Effect of common anions on the adsorption percentage.

Concentration of anions, M	Adsorption percentage in the presence of anions					
	PO_4^{3-}	SO_4^{2-}	SiO_3^{2-}	NO_3^-	HCO_3^-	PO_4^{3-}
0	99.90	99.90	99.90	99.90	99.90	99.90
0.001	54.74	99	78.89	99	99	54.74
0.01	15.23	82.24	21.78	99	54.56	15.23
0.1	1.245	44.58	5.78	67.89	23.58	1.245

When pH > 9, HAsO42- becomes dominant species of As(V) [27] and this anion may compete with negative site of the adsorbent surface to reduce the adsorption capability due to electrostatic repulsion [28]. The adsorption behavior of As(V) on IOCP is agreed with the study reported by NZVI [10]. In the pH between 4 to 7, the predominant As(V) species exists as oxyanions; $H_2AsO_4^{1-}$ and $HAsO_4^{2-}$ [26] and these ions are assumed to be adsorbed on IOCP due to Coulombic interaction [10]. The results suggest that the IOCP has a high efficiency to remove As(V) from water, and it would be a potential adsorbent to solve environmental problems.

3.4. Effect of anions on adsorption rate

The effects of common anions (HCO_3^-, SO_4^{2-}, NO_3^-, SiO_3^{2-}, and HPO_4^{2-}) coexisted in the As(V) solution were examined. The experimental conditions were kept the same under various concentrations of anions from 0 to 0.1 M. There was no significant effect on the adsorption of As(V) when the concentration increased up to 0.01 M for NO_3^- ion and 0.001 M for HCO_3^- and SO_4^{2-}(Table 3). However, when the concentration increased to 0.01 M, the adsorption percentage reduced from 99.9% to 54.56% for HCO_3^- and 82.24% for SO_4^{2-}, whereas the adsorption efficiency of SiO_3^{2-} and PO_4^{2-} ions reduced from 99.9% to 21.78% and 15.23%, respectively. While competing anion concentrations increased up to 0.1 M in As(V) solution, it decreased from 99.9% to 67.89%, 44.58%, and 23.58% for NO_3^-, SO_4^{2-}, and HCO_3^- ions, respectively; at the same concentration, the As(V) adsorption reduced from 99.9% to 1.24% for HPO_4^{2-} and to 5.78% for SiO_3^{2-}. Phosphate ion had the highest negative effect on the adsorption percentage among the anions at each concentration level. The competition of arsenic with other ionic species for the adsorptive surface sites on the adsorbent should predominantly arise from anions, especially oxyanions, due to the anionic nature of inorganic arsenic in water [27]. Because phosphate and arsenic are in the same group in the periodic table and their ionic charge and size are very similar, thus, the presence of the anions can compete with arsenic ion on the active sites of adsorbent and thus decrease the adsorption efficiency. Similar observations were also reported in the literature [28,29]. Despite the effect of these common anions, especially for phosphate and silicate ions, it is interesting to mention that these ions would not interfere with the adsorption percentage as their concentrations in natural water are usually much below than those adopted in this study.

3.5. Adsorption isotherm

Fig. 6 displays a comparison of the fitting of the experimental data with Langmuir and Freundlich adsorption isotherms. It suggests that the Langmuir model is more suitable in simulating the adsorption isotherm of As(V) onto IOCP. The related adsorption constants are listed in Table 4. The correlation coefficients of Langmuir equation (0.999) is higher than that of the Freundlich, which suggests that the adsorption belongs to the monolayer adsorption [30,31]. The adsorption rate constant is 44.84 L mg^{-1} and the maximum adsorption capacity is 0.39 mg g^{-1}.

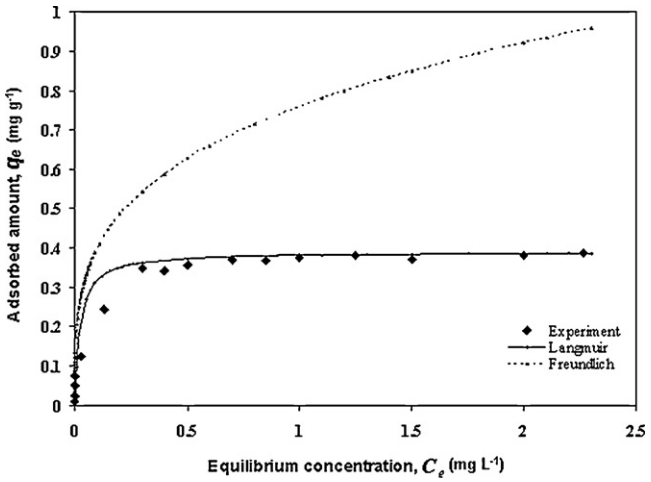

Fig. 6. The comparison of the fitting of experimental data with the adsorption isotherms of Langmuir and Freundlich equations. Reaction conditions for IOCP: 1.0 g–IOCP L^{-1} in 0.01 M NaCl at pH 6.5–7 and reaction time 24 h.

3.6. Adsorption kinetics

The experimental data were fitted to the pseudo-first-order and pseudo-second-order equations (Fig. 7). It shows that the pseudo-second-order model is more suitable for all initial As(V) concentrations, which suggests that the adsorption of As(V) onto IOCP follows pseudo-second-order kinetics. The correlation coefficients (R^2) for the pseudo-first- and pseudo-second-order equations are satisfactory (Table 5); however, the R^2 of pseudo-second-order equation is better than pseudo-first-order's. The rate constant of pseudo-second-order adsorption (K_2) ranges from 26 to 73 g mg^{-1} min^{-1} and the adsorption capacity ranges from 0.02 to 0.15 mg g^{-1} for all the initial concentrations. From the kinetic

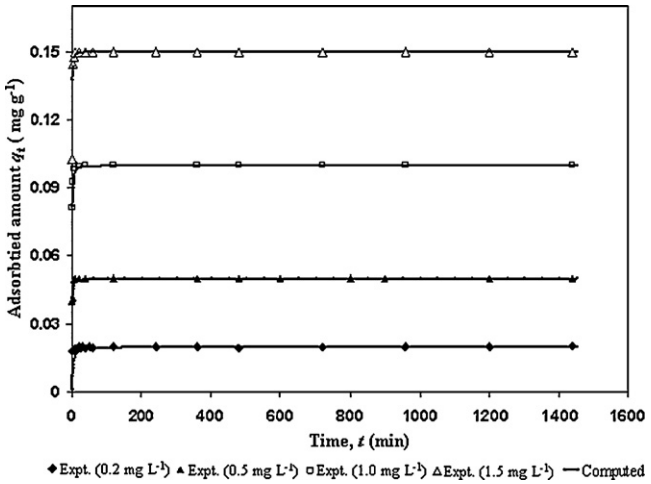

Fig. 7. Effect of initial As(V) concentrations on adsorption amount of As(V) onto IOCP with time, and the fitting of experimental data with pseudo-second-order model.

Table 4
The related parameters of Langmuir and Freundlich isotherms for As(V) adsorbed on IOCP at pH 6.5–7, temperature 30 °C, reaction time 24 h.

Langmuir model			Freundlich model		
q_m (mg g^{-1})	K (L mg^{-1})	R^2	K_F (L mg^{-1})	n	R^2
0.39	44.84	0.999	0.76	3.6	0.88

Table 5
Kinetic parameters calculated by pseudo-first-order and pseudo-second-order equations for As(V) adsorbed on IOCP.

		First-order kinetics model			Second-order kinetic model		
As(V) conc. (mg L^{-1})	q_e (expt.) (mg g^{-1})	q_e (calculated) (mg g^{-1})	K_1 (1 min^{-1})	R^2	q_e (calculated) (mg g^{-1})	K_2 (g mg^{-1} min^{-1})	R^2
0.2	0.02	0	0.20	0.9476	0.02	26.09	0.9990
0.5	0.05	0.02	0.54	0.9149	0.05	34.32	0.9997
1.0	0.10	0.03	0.58	0.9933	0.10	44.73	0.9993
1.5	0.15	0.07	0.70	0.9864	0.15	72.71	0.9999

Table 6
Comparison of iron oxide-coated perlite and other adsorbents for arsenic removal.

Adsorbent	pH	Conc. range mg L^{-1}	Temp. °C)	Model used to calculate adsorption capacity	Adsorbing capacity of As(V) mg/g	References
Iron oxide-coated sand	7.6	0.10	22 ± 2	Langmuir	0.043	Thirunavukkarasu et al. [32]
Iron oxide-coated sand IOCS-2*	7.6	0.10	22 ± 2	Freundlich	0.008	Thirunavukkarasu et al. [33]
Iron oxide coated sand (IOCS)	–	0.325	22 ± 2	Langmuir	0.018	Viraghavan et al. [34]
Al_2O_3/Fe(OH)$_3$	8.2–8.9	0.05	–	Breakthrough	0.09	Hodi et al. [35]
Iron coated zeolite (ICZ)	4	2.0	Room temp.	Langmuir	0.68	Jeon et al. [36]
Iron oxide- coated quartz (IOCQ)	6	1.5	30	Langmuir	0.097	Mostafa et al. [37]
Iron oxide- coated perlite (IOCP)	6.5–7	1.5	30	Langmuir	0.39	This study

IOCS-2* was prepared according to Benjamin et al. [38] with some modifications.

study, it indicates that As(V) is predominantly chemisorbed on the IOCP surface, which is similar to the research result of Wu et al. [22].

3.7. Comparison with other adsorbents

It has been reported that the maximum As(V) adsorption capacity of iron oxide-coated sand (IOCS), Al_2O_3/Fe(OH)$_3$, and iron coated zeolite (ICZ) are 0.008–0.043, 0.09, and 0.68 mg/g, respectively [32–37], which is listed in Table 6. In comparison, it is clear that maximum As(V) adsorption capacity of IOCP is superior to IOCS and Al_2O_3/Fe(OH)$_3$, and it is a little smaller than ICZ adsorbent. Although the adsorption capacity of arsenate onto IOCP adsorbent is lower than that of ICZ, but the main advantages of IOCP are the substantially low cost, availability of the materials, and its economic feasibility. This suggests that the adsorption property of IOCP gives the material great potential for applications in As(V) removal from aqueous streams.

3.8. Arsenate desorption

For any adsorption process, the most important factors are the reversibility and the regeneration capacity of the adsorbent. Desorption studies of the adsorbed arsenate (1 mg As(V) on 10 g IOCP) were carried out by shaking 0.5 g of As(V)-adsorbed adsorbent individually with 50 mL of 0.5 M NaOH, Na_2HPO_4 and HCl solution lasting for 24 h.

A comparison of the values with those observed in the initial sorption step was used to calculate the percentage of recovery values. About 94.52, 82.56% and 35.23% As(V) concentrations were removed from the IOCP surface after the reaction at 24 h of for HCl, NaOH and Na_2HPO_4, respectively (Fig. 8). Thus HCl was more capable to act as an efficient eluant, however, it would destroy the IOCP surface. Therefore NaOH would be preferable to use in the regeneration experiment. Theis et al. (1992) reported that a slower desorption rate of cadmium from goethite suggested the reaction mechanism involved chemical reactivity. The results of this study also showed a slower desorption rate in comparison with the adsorption step, thus the evidence indicating the chemical bonding was formed between arsenic ions and the coated surfaces.

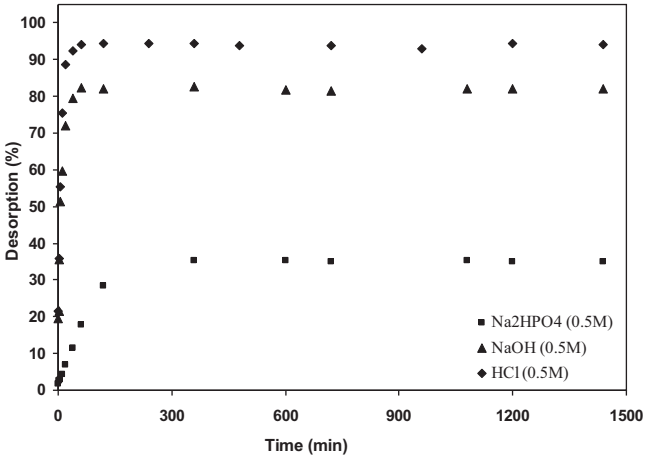

Fig. 8. Desorption of As(V) on IOCP as a function of time. Reaction conditions: 10 g/L As(V) adsorbed IOCP in HCl, NaOH and Na_2HPO_4 solution (0.5 M) at 30 °C and reaction time around 24 h.

4. Conclusion

In summary, BET results suggest that the IOCP has more micropores and higher specific surface areas. EDAX and FT-IR analyses reveal that the arsenate can be adsorbed onto iron oxide-coated perlite. Besides, the results show that arsenic ions are chemisorbed

on the surface of IOCP. The adsorption rate of As(V) is very fast and equilibrium time is around 5 min. About 100% of As(V) removal is achieved within 5 min from the samples containing initial As concentration up to 1.5 mg L^{-1}. Moreover, IOCP has the potential to adsorb As(V) over a wide pH range. Common anions, like sulfate, phosphate, carbonate nitrate, and silicate, do not obstruct the adsorption behavior at the level of their concentrations present in groundwater. It is also observed that the experimental results of adsorption isotherms are well fitted with the Langmuir model and the maximum adsorption capacity is 0.39 mg g^{-1}. The pseudo-second-order model is more suitable for all initial As(V) concentrations, suggesting that the adsorption of As(V) onto IOCP follows pseudo-second-order kinetics. From the desorption experiment, it suggests that NaOH will be a potential eluant for the removal of arsenate from the adsorbed IOCP surface. Thus, IOCP would be a potential adsorbent at neutral pH for the arsenic removal from water.

Acknowledgements

The authors are thankful to the Top 100 Universities Advancement Office for the financial support. We greatly appreciate Mr. Hung-Yuan Huang of Instrument Precision Center for ESEM-EDAX analyses, Dr. W.-T. Jiang, Mr. G.-T. Hung and Dr. C.-J. Wang (Micro-Nano-Mineral Science Group of Earth Science Department at National Cheng Kung University) for XRD analysis.

References

[1] P.L. Smedley, D.G. Kinniburgh, A review of the source, behaviour and distribution of arsenic in natural waters, Appl. Geochem. 17 (2002) 517–568.
[2] A. Demirbas, Heavy metal adsorption onto agrobased waste materials: a review, J. Hazard. Mater. 157 (2008) 220–229.
[3] D. Sud, G. Mahajan, M.P. Kaur, Agricultural waste material as potential adsorbent for sequestering heavy metal ions from aqueous solutions—a review, Bioresour. Technol. 99 (2008) 6017–6027.
[4] S.P. Singh, L.Q. Ma, M.J. Hendry, Characterization of aqueous lead removal by phosphatic clay: equilibrium and kinetic studies, J. Hazard. Mater. 136 (2006) 654–662.
[5] V.K. Gupta, V.K. Saini, N. Jain, Adsorption of As(III) from aqueous solutions by iron oxide-coated sand, J. Colloid Interface Sci. 288 (2005) 55–60.
[6] G. Zhang, J. Qu, H. Liu, R. Liu, R. Wu, Preparation and evaluation of a novel Fe–Mn binary oxide adsorbent for effective arsenite removal, Water Res. 41 (2007) 1921–1928.
[7] M.M. Benjamin, J.O. Leckie, Multiple-site adsorption of cadmium, copper, zinc, and lead on amorphous iron oxyhydroxide, Colloid Interface Sci. 79 (1981) 209–221.
[8] S Schwertmann, R.M. Taylor, Iron oxides. Minerals in soil environments, in: J.B. Dixon, S.B. Weed (Eds.), Soil Sci. Soc. Am. J., 2nd ed., Madison, Wisconsin, 1989, pp. 379–428.
[9] S. Dixit, J.G. Hering, Effects of arsenate reduction and iron oxide transformation on arsenic mobility, Environ. Sci. Technol. 37 (2003) 4182–4189.
[10] S.R. Kanel, J.-M. Grene, H.-C. Choi, Arsenic(V) removal from groundwater using nano scale zero-valent iron as a colloidal reactive barrier material, Environ. Sci. Technol. 40 (2006) 2045–2050.
[11] L.A. Zeng, A mothod for preparing silica-containing iron(III) oxide adsorbents for arsenic removal, Water Res. 37 (2003) 4351–4358.
[12] T.L. Theis, R. Iyer, S.K. Ellis, Evaluating a new granular iron oxide for removing lead from drinking water, J. AWWA 84 (1992) 101–105.
[13] M. Alkan, M. Doğan, Perlite Surfaces. Encyclopedia of Surface and Colloid Science, Marcel Dekker, New York, 2002, pp. 3945–3958.
[14] M. Dogan, M. Alkan, Y. Onganer, Adsorption of methylene blue from aqueous solution onto perlite, Water Air Soil Pollut. 120 (2000) 229–248.
[15] K. Swayampakulaa, V.M. Boodu, S.K. Nadavala, K. Abburia, Competitive adsorption of Cu (II), Co (II) and Ni (II) from their binary and tertiary aqueous solutions using chitosan-coated perlite beads as biosorbent, J. Hazard. Mater. 170 (2009) 680–689.
[16] S. Hasan, A. Krishnaiah, T.K. Ghosh, V.M. Boodu, E.D. Smith, Chromium (VI) adsorption capacity of chitosan coated on an inert substrate perlite, Sep. Sci. Technol. 38 (2003) 3375–3393.
[17] A. Kalyani, J. Ajitha Priya, P.S. Rao, A. Krishnaiah, Removal of copper and nickel from aqueous solutions using chitosan coated on perlite as biosorbent, Sep. Sci. Technol. 40 (2005) 1483–1495.
[18] D. Kratochvil, B. Volesky, G. Demopoulos, Optimizing Cu removal/recovery in a biosorption column, Water Res. 31 (1997) 2327–2339.
[19] Z. Talip, M. Eral, U. Hicsonmez, Adsorption of thorium from aqueous solutions by perlite, J. Environ. Radioact. 100 (2009) 139–143.
[20] H.S. Teng, J.-A. Ho, Y.-F. Hsu, C.-T. Hsieh, Preparation of activated carbons from bituminous coals with CO_2 activation, Ind. Eng. Chem. Res. 35 (1996) 4043–4049.
[21] Z. Aksu, G. Donmez, A comparative study on the biosorption characteristics of some yeasts for remazol blue reactive dye, Chemosphere 50 (2003) 1075–1083.
[22] F.-C. Wu, R.-L. Tseng, R.-S. Juang, Kinetic modeling of liquid-phase adsorption of reactive dyes and metal ions on chitosan, Water Res. 35 (2001) 613–618.
[23] Y.S. Ho, G. McKay, Comparisons of chemisorption kineticmodels applied to pollutant removal on various sorbents, Trans. Inst. Chem. Eng. 76B (1998) 332–340.
[24] Y.S. Ho, D.A.J. Wase, C.F. Forster, Study of the sorption of divalent metal ions on to peat, Adsorption Sci. Technol. 18 (2000) 639–650.
[25] X.-H. Guan, J. Wang, C.C. Chusuei, Removal of arsenic from water using granular ferric hydroxide: macroscopic and microscopic studies, J. Hazard. Mater. 156 (2008) 178–185.
[26] R.S. Oremland, J.F. Stolz, The ecology of arsenic, Science 300 (2003) 939–944.
[27] C. Su, R.W. Puls, Arsenate and arsenite removal by zerovalent iron: effects of phosphate, silicate, carbonate, borate, sulfate, chromate, molybdate and nitrate, relative to chlorine, Environ. Sci. Technol. 35 (2001) 4562–4568.
[28] Z. Cheng, A. Van Geen, R. Louis, N. Nikolaidis, R. Bailey, Removal of methylated arsenic in groundwater with iron filings, Environ. Sci. Technol. 39 (2005) 7662–7666.
[29] T. Radu, J.L. Subacz, J.M. Phillippi, M.O. Barnett, Effects of dissolved carbonate on arsenic adsorption and mobility, Environ. Sci. Technol. 39 (2005) 7875–7882.
[30] R.-S. Juang, S.-L. Swei, Effect of dye nature on its adsorption from aqueous solutions onto activated carbon, Sep. Sci. Technol. 31 (1996) 2143–2158.
[31] D. Mohapatra, D. Mishra, G.R. Chaudhury, R.P. Das, Arsenic adsorption mechanism on clay minerals and its dependence on temperature, Korean J. Chem. Eng. 24 (2007) 426–430.
[32] O.S. Thirunavukkarasu, T. Virghavan, K.S. Suramanian, Arsenic removal from drinking water using iron oxide-coated sand, Water Air Soil Pollut. 142 (2003) 95–111.
[33] O.S. Thirunavukkarasu, T. Virghavan, K.S. Suramanian, S. Tanjore, Organic arsenic removal from drinking water, Urban Water 4 (2002) 415–421.
[34] T. Virghavan, O.S. Thirunavukkarasu, K.S. Suramanian, Removal of arsenic in drinking water by iron oxide-coated sand and ferrihydrite – batch studies, Water Qual. Res. J. Can. 36 (2001) 55–70.
[35] M. Hodi, K. Polyak, J. Hlavay, Removal of pollutants from drinking water by combined Ion exchange and adsorption method, Environ. Int. 21 (1995) 325–331.
[36] C.-S. Jeon, K. Baek, J.-K. Park, Y.-K. Oh, S.-D. Lee, Adsorption characteristics of As(V) on iron-coated zeolite, J. Hazard. Mater. 163 (2009) 804–808.
[37] M.G. Mostafa, Y.-H. Chen, J.-S. Jean, C.-C. Liu, H. Teng, Adsorption and desorption properties of arsenic onto nano-sized iron oxide-coated quartz, Water Sci. Technol. (2010).
[38] M.M. Benjamin, R.S. Sletten, R.P. Bailey, T. Bennet, Water Res. 30 (1996) 2609–2620.